



3-(Substituted Aryl/alkyl)-5-((E)-4-((E)-(Substituted Aryl/alkyl)methyl)benzylidene)thiazolidin-2,4-dione Molecules: Design, ADME Studies and Molecular Docking Analysis as Potential Antimicrobial and Antiproliferative Agents

HARSH KUMAR^{1,✉}, AASTHA SHARMA^{1,✉}, DAVINDER KUMAR^{1,✉}, MINAKSHI GUPTA MARWAHA^{2,✉} and RAKESH KUMAR MARWAHA^{1,*,✉}

¹Department of Pharmaceutical Sciences, Maharshi Dayanand University, Rohtak-124001, India

²Department of Pharmaceutical Sciences, Sat Priya College of Pharmacy, Rohtak-124001, India

*Corresponding author: E-mail: rkmarwaha.mdu@gmail.com

Received: 23 May 2022;

Accepted: 8 July 2022;

Published online: 19 August 2022;

AJC-20939

A library comprising of 60 synthesizable compounds from three different series having 20 compounds in each series of 3-(furan-2-carbonyl)-5-((E)-4-((E)-(substituted aryl/alkyl)methyl)benzylidene)thiazolidine-2,4-dione (**FC-1** to **FC-20**), 3-(butyl)-5-((E)-4-((E)-(substituted aryl/alkyl)methyl)benzylidene)thiazolidine-2,4-dione (**NB-1** to **NB-20**) and 3-(allyl)-5-((E)-4-((E)-(substituted aryl/alkyl)methyl)benzylidene)thiazolidine-2,4-dione (**NA-1** to **NA-20**) was designed and screened for antimicrobial and anticancer potential by molecular docking studies using *S. aureus* GyrB ATPase (PDB code: 3U2D) and CDK-8 (PDB code: 5FGK) proteins as possible drug targets, respectively by Schrödinger-Maestro v13.2. Molecular docking studies revealed, analogues **NB-3** (docking score = -6.626), **NA-3** (docking score = -6.315) and **FC-20** (docking score = -5.552) displayed best docking score in each series, respectively against 3U2D and molecules **NB-2** (docking score = -6.517), **NA-20** (docking score = -7.668) and **FC-12** (docking score = -4.931) exhibited best docking score in each series, respectively against 5FGK having better interaction with crucial amino acid. ADME results revealed all the analogues have significant scores within Qikprop range and also in close agreement with the Pfizer's rule of five. These analogues can be used as lead structures for the development/discovery of new anticancer and antimicrobial agents.

Keywords: Thiazolidine-2,4-diones, Antimicrobial, Anticancer, CDK-8, GyrB ATPase, Molecular docking, ADME.

INTRODUCTION

Drug development process is very costly, multifaceted and long process that may take 12-15 years of time to obtain a drug candidate from thousands of compounds which can be used to treat a disease. Molecular docking, an *in-silico* computational approach, is now a days attaining popularity due its ability to the study complex biological system, prediction of binding affinity of drug molecule to a specific targeted site (protein/enzyme, etc.) and its biological response. Therefore, can be of great value in developing and identifying the new lead compound with higher success rate [1,2]. Poor pharmacokinetic properties (ADME) are among the major reasons for drug failure found by the researchers and contribute approximately 40% of drug failure during drug development process and hence leads to significant escalation in the cost of drug development [3]. Now a days, it has been realized that optimization of ADME

properties of a drug molecules is an important task for reducing the chances of drug failure [4] and ultimately the cost of drug molecule.

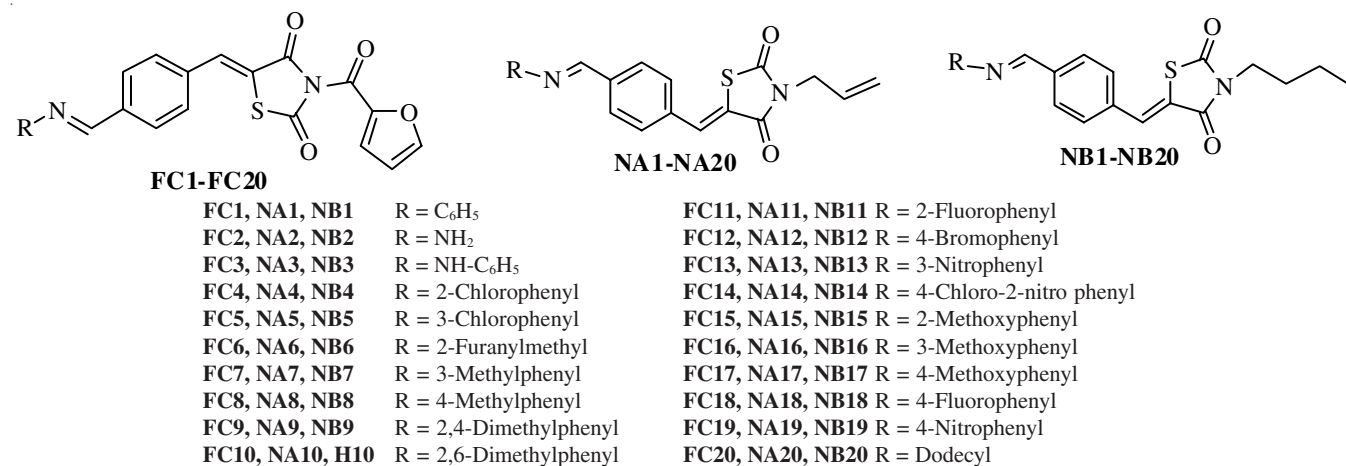
In recent years, due to the increased rate of resistance for currently available antibacterial drugs against Gram-positive as well as Gram-negative pathogens like Methicillin resistant *S. aureus* (MRSA), are considered to be a life-threatening issue [5]. The rapid adaptation of microorganism to antibiotics, higher mortality and low number of newly approved drugs have created a high demand and challenge for researchers to discover novel drugs for treatment of diseases [6].

DNA gyrase, a protein of topoisomerase-II class is essentially required for the replication, transcription and recombination in bacteria [7]. It is identified as target for antibacterial drugs due to its absence in human beings [8]. It plays a key role in ATP-dependent negative supercoiling of DNA strands. DNA gyrase also play a crucial role in chromosomal segre-

gation. It exists in two forms *i.e.* Gyrase A and Gyrase B and inhibition of these targeted enzyme leads to modulation in DNA topology [9]. The various formulations of DNA gyrase inhibitors belonging to different chemical classes such as amino coumarins (novobiocin), quinolones (nalidixic acid) and Fluoroquinolones (ciprofloxacin, ofloxacin, levofloxacin), *etc.* are widely used as antibacterial agents [7]. Inhibiting these targeted enzymes can be explored to build more efficient antibacterial target and improve the efficiency of the existing marketed drugs [10].

Protein kinases is considered to be the most significant class of enzymes due to its significant role in cell cycle progression, cell division and cell proliferation [11]. Recent studies have revealed that during the stressful activities such as heat shock, the kinase activity is necessary for the gene activation [12]. Cyclin dependent kinase (CDK), a kinase module subunit of mediator complex in eukaryotes, plays an important role in transcriptional regulation. Specifically, a canonical holo-mediator complex comprises of four parts *i.e.* head, middle, tail and CDK. The CDK comprises of CDK-8 and CDK-19 subunits and plays opposite role to each other in transcription regulation [13]. The CDK-8 regulates RNA polymerase II transcriptional machinery by mediating suppressive as well activating gene expression by carry signals from repressors and activators. It also considered as a potent oncoprotein in colorectal cancer [14]. As a part of mediator complex, it has role in innate immunity, homeostasis and in developmental signaling. Interruption in these complex leads to face a serious health issue like cancer [15]. As a co-activator, it promotes gene expression in various molecular pathway like β -catenin pathway/WNT signaling pathway, p53 pathway, thyroid hormone dependent pathway and others. It causes various health disorders like inflammatory, degenerative and malignant disorders. In sum, it serves its role in cancer associated problems and might be act as good targeting site [16].

In present study, we hereby account for designing, molecular docking studies and ADME parameters of 3,5-disubstituted thiazolidin-2,4-dione derivatives that helps in studying the interaction of target site and designed molecules. The designed molecules with best docking score can be further taken up for synthesis and *in vitro* studies.



Scheme-I: Structures of designed molecules

EXPERIMENTAL

Present work has been carried out on HP Pavilion 15-cc129 Intel(R) Core™ i5-8250U CPU@1.60GHz 1.80 GHz.

Data set: A library comprising of 3 different series having 60 synthesizable compounds (20 compounds in each series) of 3-(furan-2-carbonyl)-5-((*E*)-4-((*E*)-(substituted aryl/alkyl)methyl)benzylidene)thiazolidine-2,4-dione (**FC-1** to **FC-20**), 3-(butyl)-5-((*E*)-4-((*E*)-(substituted aryl/alkyl)methyl)benzylidene)thiazolidine-2,4-dione (**NB-1** to **NB-20**) and 3-(allyl)-5-((*E*)-4-((*E*)-(substituted aryl/alkyl)methyl)benzylidene)thiazolidine-2,4-dione (**NA-1** to **NA-20**) was designed by modifying the molecules of earlier study reported by Kumar *et al.* [17]. The structures of the designed molecules were drawn by using ChemDraw Ultra software 15.0. The structures of the data set molecules are shown in **Scheme-I**.

ADME studies: Drug likeness/ compound druggability can be assessed by Lipinski's (or Pfizer's) rule of five [18], which can determine a drug molecule to be orally active in humans based on their chemical/physical properties having certain biological/pharmacological activities [19]. Lipinski's rule of five states that (i) hydrogen bond donors ≤ 5 , (ii) hydrogen bond acceptors ≤ 10 , (iii) molecular mass ≤ 500 Daltons, (iv) an octanol-water partition coefficient ≤ 5 . Schrödinger software 2022-1 (Maestro version 13.2) having QikProp module was used for the calculation of ADME parameters [20]. Around eleven physical parameters having certain pharmacological properties were analyzed using Qikprop module. The ADME studies results revealed that most of the designed molecules exhibited the significant results within the limits of Lipinski's rule of five and within the range Qikprop module *i.e.* molecular weight of the molecule (mol. MW ≤ 500), predicted water/gas partition coefficient (QPlogK_p = -8.0 to -1.0), (QPlogP_w = 4.0 to -45.0), predicted octanol/water partition coefficient (QPlogP_{o/w} = -2.0 to -6.5), predicted brain/blood partition coefficient (QPlog BB = -3.0 to -1.2), donor HB (0.0 to -6.0), accept HB (2.0 to -20.0), percent human oral absorption (0 to 100), human oral absorption (1, 2 or 3). The ADME results are shown in Table-1.

Molecular docking

Preparation of protein/macromolecule structures: The structures of the target proteins *i.e.* *S. aureus* GyrB ATPase

TABLE-1
ADME PARAMETERS OF MOLECULES FC-1 TO FC-20, NA-1 TO NA-20 AND NB-1 TO NB-20

Comp.	m.w.	Rule of five	QPlog Po/w	Human oral absorption	Volume	% Human oral absorption	QPlog P _w	QPlog K _p	QPlog BB	Donor HB	Accept HB
FC-1	402.424	0	4.056	3	1223.925	100	10.808	-1.366	-0.996	0	6.5
FC-2	341.341	0	1.366	3	1012.872	71.942	13.641	-3.606	-1.701	2	7.5
FC-3	417.438	0	3.686	3	1267.818	96.834	13.713	-1.563	-1.267	1	8.0
FC-4	436.869	0	4.53	3	1266.365	100	10.581	-1.493	-0.843	0	6.5
FC-5	436.869	0	4.565	1	1268.961	100	10.575	-1.538	-0.851	0	6.5
FC-6	406.412	0	3.507	3	1225.315	100	11.231	-1.48	-1.081	0	7.5
FC-7	416.45	0	4.383	3	1284.343	100	10.511	-1.566	-1.033	0	6.5
FC-8	416.45	0	4.383	3	1283.549	100	10.503	-1.553	-1.023	0	6.5
FC-9	430.477	0	4.692	1	1338.493	100	10.209	-1.705	-1.02	0	6.5
FC-10	430.477	0	4.668	1	1329.766	100	10.227	-1.613	-0.961	0	6.5
FC-11	420.414	0	4.285	3	1240.023	100	10.608	-1.467	-0.891	0	6.5
FC-12	481.32	0	4.64	1	1277.005	100	10.577	-1.538	-0.839	0	6.5
FC-13	447.421	0	3.301	3	1297.324	80.707	11.932	-3.283	-2.193	0	7.5
FC-14	481.866	0	3.866	3	1330.419	87.104	11.572	-3.097	-1.804	0	7.5
FC-15	432.45	0	4.155	3	1303.144	100	11.067	-1.429	-1.08	0	7.25
FC-16	432.45	0	4.12	3	1298.9	100	11.042	-1.45	-1.077	0	7.25
FC-17	432.45	0	4.122	3	1299.174	100	11.038	-1.449	-1.078	0	7.25
FC-18	420.414	0	4.295	3	1239.696	100	10.586	-1.494	-0.887	0	6.5
FC-19	447.421	0	3.304	3	1297.232	80.813	11.932	-3.272	-2.188	0	7.5
FC-20	494.648	1	6.717	1	1711.033	100	8.282	-1.22	-1.908	0	7.0
NA-1	348.419	0	4.898	3	1143.708	100	7.036	-0.921	-0.602	0	4
NA-2	287.336	0	2.192	3	932.361	83.511	9.862	-3.155	-1.313	2	5
NA-3	363.433	0	4.394	3	1186.958	100	9.938	-1.117	-0.857	1	5.5
NA-4	382.864	1	5.363	1	1185.084	100	6.799	-1.056	-0.445	0	4
NA-5	382.864	1	5.404	1	1187.937	100	6.797	-1.088	-0.444	0	4
NA-6	352.407	0	4.336	3	1141.873	100	7.454	-1.015	-0.666	0	5
NA-7	362.445	1	5.228	1	1204.55	100	6.738	-1.124	-0.63	0	4
NA-8	362.445	1	5.234	1	1204.804	100	6.738	-1.112	-0.624	0	4
NA-9	376.472	1	5.541	1	1258.269	100	6.431	-1.244	-0.602	0	4
NA-10	376.472	1	5.515	1	1249.779	100	6.454	-1.162	-0.559	0	4
NA-11	366.409	1	5.125	3	1159.209	100	6.833	-1.018	-0.493	0	4
NA-12	427.315	1	5.483	1	1196.792	100	6.807	-1.092	-0.435	0	4
NA-13	393.416	0	4.149	3	1217.595	92.397	8.161	-2.83	-1.754	0	5
NA-14	427.861	0	4.717	1	1250.903	100	7.815	-2.64	-1.378	0	5
NA-15	378.445	1	5.007	3	1223.842	100	7.3	-0.976	-0.673	0	4.75
NA-16	378.445	0	4.957	3	1221.014	100	7.25	-1.065	-0.7	0	4.75
NA-17	378.445	0	4.966	3	1220.671	100	7.282	-1.031	-0.693	0	4.75
NA-18	366.409	1	5.14	3	1160.352	100	6.82	-1.057	-0.497	0	4
NA-19	393.416	0	4.154	3	1217.953	92.487	8.16	-2.824	-1.751	0	5
NA-20	440.643	1	7.584	1	1625.588	100	4.461	-0.613	-1.318	0	4.5
NB-1	364.461	1	5.345	1	1221.943	100	6.645	-1.013	-0.718	0	4
NB-2	303.378	0	2.588	3	1009.621	85.402	9.475	-3.253	-1.465	2	5
NB-3	379.476	0	4.815	1	1264.751	100	9.546	-1.212	-0.98	1	5.5
NB-4	398.906	1	5.823	1	1263.676	100	6.411	-1.117	-0.549	0	4
NB-5	398.906	1	5.85	1	1266.374	100	6.408	-1.185	-0.564	0	4
NB-6	368.45	0	4.781	3	1216.835	100	7.043	-1.053	-0.751	0	5
NB-7	378.488	1	5.672	1	1282.495	100	6.344	-1.216	-0.745	0	4
NB-8	378.488	1	5.668	1	1282.179	100	6.347	-1.221	-0.748	0	4
NB-9	392.515	1	5.984	1	1336.571	100	6.042	-1.346	-0.723	0	4
NB-10	392.515	1	5.951	1	1327.667	100	6.062	-1.274	-0.682	0	4
NB-11	382.452	1	5.581	1	1237.633	100	6.444	-1.088	-0.6	0	4
NB-12	443.357	1	5.929	1	1274.898	100	6.414	-1.183	-0.551	0	4
NB-13	409.459	0	4.591	1	1295.61	94.577	7.77	-2.93	-1.913	0	5
NB-14	443.904	1	5.153	1	1328.669	87.911	7.412	-2.753	-1.53	0	5
NB-15	394.487	1	5.447	1	1301.563	100	6.901	-1.075	-0.79	0	4.75
NB-16	394.487	1	5.404	1	1296.938	100	6.88	-1.112	-0.799	0	4.75
NB-17	394.487	1	5.413	1	1298.573	100	6.886	-1.115	-0.805	0	4.75
NB-18	382.452	1	5.582	1	1237.785	100	6.427	-1.147	-0.611	0	4
NB-19	409.459	0	4.592	1	1295.334	94.634	7.767	-2.924	-1.909	0	5
NB-20	456.685	1	8.02	1	1698.74	100	4.06	-0.648	-1.393	0	4.5

(PDB Id: 3U2D) with 1.85 Å resolution and human cyclin-dependent kinase CDK-8 (PDB: 5-FGK) with 2.36 Å identified from literature were retrieved from Protein Data Bank. The structures were then prepared using Protein Preparation Wizard module of Schrödinger 2022-1 (Maestro version 13.2) using default parameters *i.e.* (i) pre-process, which took care of missing hydrogen molecules and missing amino acids; (ii) optimize the H-bond assignment, which adjust the orientation of the hydrogen molecules of water molecules and amino acids and hence H-bond network followed by (iii) clean up, which minimizes the energy and also delete the water molecules which are far away from ligand molecules. Energy minimization was done using OPLS4 force field with a root mean square deviation (RMSD) value of 0.30 Å.

Ligand structure preparation: The structures of ligands were optimized using LigPrep module Schrödinger 2022-1 (Maestro version 13.2) [21]. The structures of the ligands were loaded by clicking the “file” option followed by “import structure” option to load the files of ligands on to the workspace. The ligands were then prepared by using the OPLS4 force field, which generates various conformations of each ligand. The stable conformer with minimum energy of every ligand was further treated for molecular docking.

Receptor grid generation: The grid generation was done to identify the binding pocket and also to generate grid which is further used for docking. Receptor Grid Generation module of Glide tool [22] of Schrödinger 2022-1 (Maestro version 13.2). Generation of grid box was done by selecting any atom of the active site. The grid of 30 Å × 30 Å × 30 Å size was selected for grid generation.

Molecular docking: Docking module of Glide tool [23] of Schrödinger 2022-1 (Maestro version 13.2) was employed to dock the prepared ligands in the identified binding site of

protein grid. The interaction of receptor and ligand was visualized using XP precision mode with default parameters for each docking run having lowest binding pose energy. The interactions of receptor-ligands were analyzed along with scoring functions [24-26].

RESULTS AND DISCUSSION

The docking results were screened for all ligands to analyze the binding mode in the binding pockets of target proteins *i.e.* *S. aureus* GyrB ATPase (PDB Id: 3U2D) with R-value free (0.232) and human cyclin-dependent kinase CDK-8 (PDB: 5-FGK) with R-value free (0.237). The results of docking analysis showed good interactions with crucial amino acids in the ATP binding pocket of the proteins (Table-2). The molecular docking results described in terms of negative energy for each ligand. The best is the binding affinity for the receptor for any ligand which is having low binding energy value [27]. Molecular docking analysis results revealed that the molecules having alkyl substitution at 3rd position exhibited better docking score in comparison to aryl substituted compounds at 3rd position. Further docking analysis with 3U2D protein revealed that molecules **NB-3** (docking score = -6.626), **NB-20** (docking score = -6.179), **NB-14** (docking score = -5.829); **NA-3** (docking score = -6.315), **NA-20** (docking score = -5.858), **NA-18** (docking score = -5.655); **FC-20** (docking score = -5.552), **FC-4** (docking score = -4.353) and **FC-1** (docking score = -4.218) exhibited best score in each series respectively. If we look into the binding mode of these molecules with 3U2D protein, it is found that the NH of thiazolidin-2,4-dione form hydrogen bonding with amino acid ASP81 of protein in most of the molecules. The binding residues of protein interact with the most active ligands along with docking score as displayed in Table-3. The ligand interaction (2D) and binding surface (3D) images of most

TABLE-2
In silico DOCKING SCORE OF THE MOLECULES FC-1 TO FC-20, NA-1 TO NA-20
AND NB-1 TO NB-20 WITH 3U2D PROTEIN AND 5FGK PROTEIN

Compd.	3U2D	5FGK	Compd.	3U2D	5FGK	Compd.	3U2D	5FGK
FC-1	-4.218	-4.149	NA-1	-5.337	-4.822	NB-1	-5.343	-5.902
FC-2	-2.3	-4.164	NA-2	-4.615	-7.146	NB-2	-4.645	-6.517
FC-3	-0.817	-1.96	NA-3	-6.315	-5.803	NB-3	-6.626	-4.561
FC-4	-4.353	-3.567	NA-4	-5.551	-6.002	NB-4	-5.300	-5.846
FC-5	0.462	-2.101	NA-5	-5.614	-4.588	NB-5	-5.307	-6.286
FC-6	-1.278	-0.52	NA-6	-3.186	-3.744	NB-6	-2.940	-4.215
FC-7	-1.777	-4.629	NA-7	-4.663	-6.078	NB-7	-5.213	-4.998
FC-8	-3.551	-1.859	NA-8	-4.395	-6.118	NB-8	-4.429	-5.027
FC-9	-0.193	-4.8	NA-9	-5.078	-6.07	NB-9	-4.443	-6.169
FC-10	-1.465	-3.262	NA-10	-4.568	-4.861	NB-10	-4.961	-4.971
FC-11	-2.297	-4.82	NA-11	-5.630	-4.721	NB-11	-5.607	-5.986
FC-12	-2.974	-4.931	NA-12	-4.415	-4.066	NB-12	-4.234	-6.502
FC-13	-3.617	-2.102	NA-13	-4.616	-6.12	NB-13	-4.544	-6.368
FC-14	-3.371	-3.51	NA-14	-5.554	-6.141	NB-14	-5.829	-3.861
FC-15	-3.948	-2.751	NA-15	-5.536	-4.958	NB-15	-5.448	-6.444
FC-16	-1.516	-0.743	NA-16	-5.651	-4.514	NB-16	-5.827	-6.493
FC-17	-3.506	-2.652	NA-17	-5.021	-5.785	NB-17	-4.568	-5.582
FC-18	-3.655	-4.343	NA-18	-5.655	-4.759	NB-18	-5.422	-5.993
FC-19	-1.755	-3.243	NA-19	-4.195	-5.206	NB-19	-3.926	-5.675
FC-20	-5.552	-1.151	NA-20	-5.858	-7.668	NB-20	-6.179	-6.023
Std.	-5.107	-4.015	Std.	-5.107	-4.015	Std.	-5.107	-4.015

active compounds of each series along with standard drugs are displayed in Fig. 1.

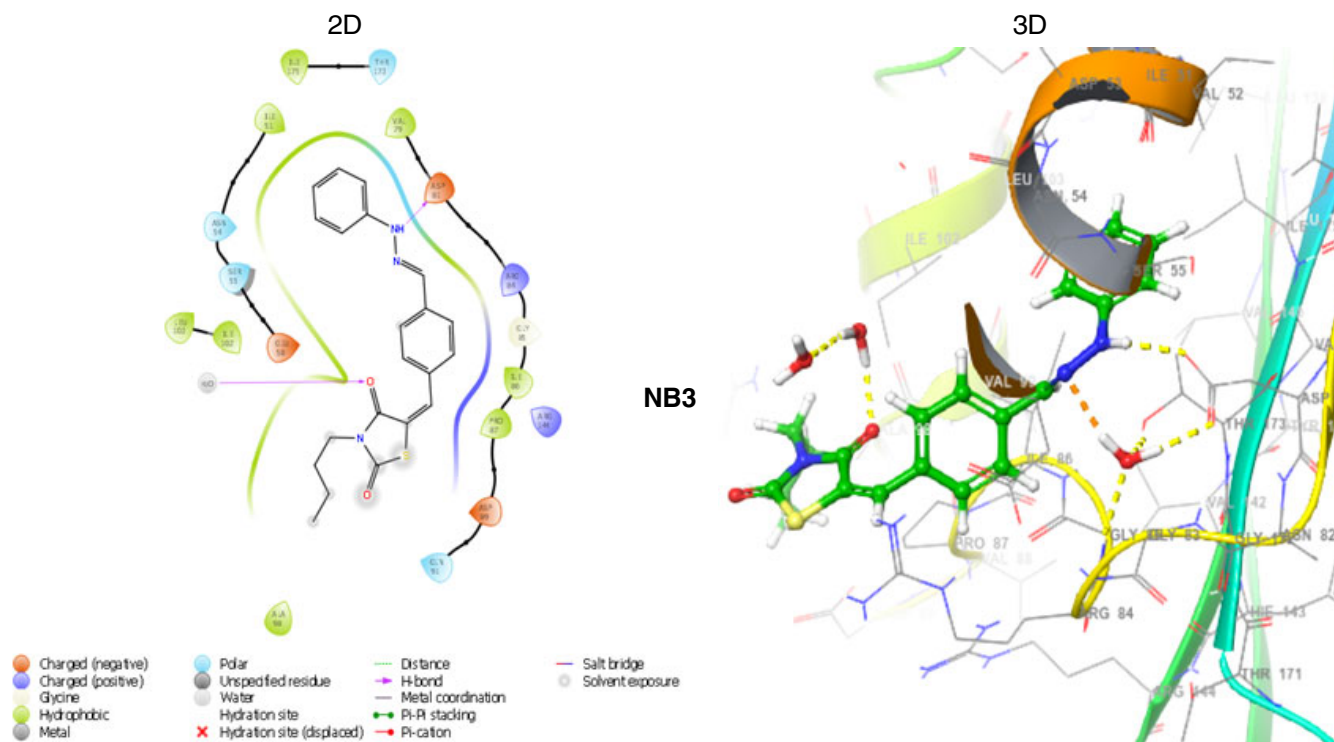
In case of 5FGK protein, the molecules **NB-2** (docking score = -6.517), **NB-12** (docking score = -6.502), **NB-16** (docking score = -6.493); **NA-20** (docking score = -7.668), **NA-2** (docking score = -7.146), **NA-14** (docking score = -6.141); **FC-12** (docking score = -4.931), **FC-11** (docking score = -4.820) and **FC-9** (docking score = -4.800) demonstrated best score in each series. The binding mode of 5FGK protein with best docked molecule **NA-20** developed pi-pi staking with TYR32 amino acid; oxygen of thiazolidine ring form hydrogen bond with ALA100

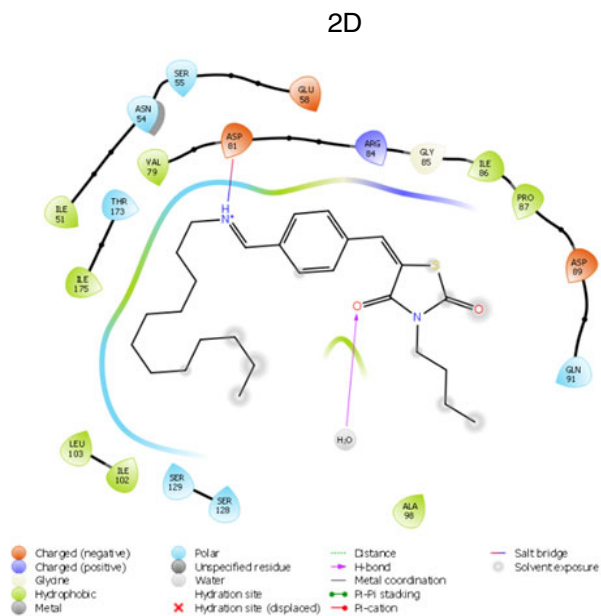
and NH of schiff's base prepare hydrogen bond with ASP 173 amino acid, respectively. Most of the other molecules exhibited formation of hydrogen bond with ALA100 amino acids with oxygen of thiazolidine ring. The binding residues of protein interact with the most active ligands along with docking score is given in Table-4. The ligand interaction (2D) and binding surface (3D) images of most active compounds of each series along with standard drugs are displayed in Fig. 2.

The molecular docking results revealed that the molecules having alkyl substitution (butyl/allyl) at 3rd position exhibited good score comparable or more potent than standard drugs

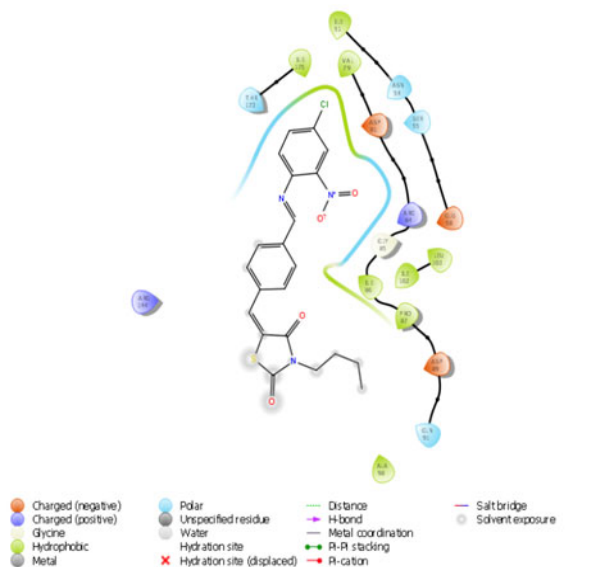
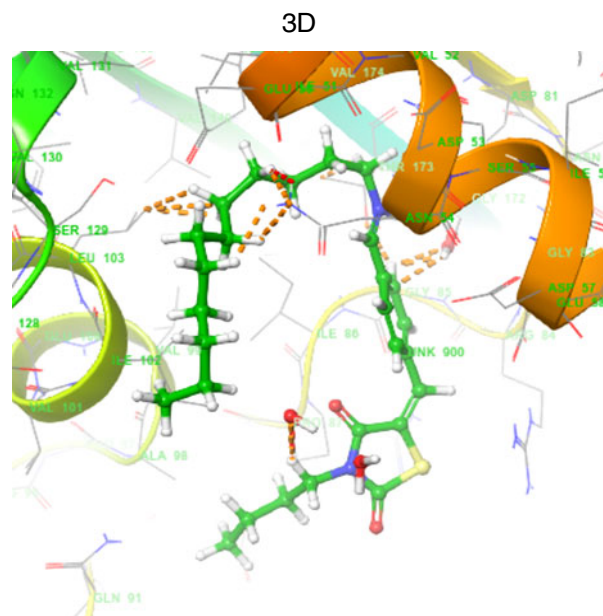
TABLE-3
DOCKING SCORE AND INTERACTIONS OF MOST ACTIVE COMPOUNDS ALONG WITH STANDARD DRUG OFLOXACIN IN THE BINDING POCKET OF 3U2D PROTEIN

Compound	Docking score	Interacting residues
NB-3	-6.626	ASP89, PRO87, ILE86, GLY85, ARG84, ASP81, THR173, ILE175, ILE51, ASN54, SER55, GLU58, LEU103, ILE102, VAL79, GLN91, ALA98, ARG144
NA-3	-6.315	ASP89, PRO87, ILE86, GLY85, ARG84, GLY83, ASP81, THR173, ILE175, ILE51, ASN54, SER55, GLU58, LEU103, ILE102, VAL79, GLN91, ALA98, ARG144
NB-20	-6.179	ASP89, PRO87, ILE86, GLY85, ARG84, ASP81, THR173, ILE175, ILE51, ASN54, SER55, GLU58, LEU103, ILE102, VAL79, GLN91, ALA98, SER128, SER129
NA-20	-5.858	PRO87, ILE86, GLY85, ARG84, ASP81, THR173, ILE175, ILE51, ASN54, SER55, GLU58, LEU103, ILE102, VAL79, ARG144, SER129, VAL130, VAL131
NB-14	-5.829	ASP89, PRO87, ILE86, GLY85, ARG84, ASP81, THR173, ILE175, ILE51, ASN54, SER55, GLU58, LEU103, ILE102, VAL79, GLN91, ALA98, ARG144
NA-18	-5.655	ASP89, PRO87, ILE86, GLY85, ARG84, ASP81, THR173, ILE175, ILE51, ASN54, SER55, GLU58, ILE102, VAL79, ALA98, ARG144
FC-20	-5.552	PRO87, ILE86, GLY85, ARG84, ASP81, THR173, ILE175, ILE51, ASN54, SER55, GLU58, LEU103, ILE102, VAL79, SER128, SER129, VAL130, ARG144
FC-4	-4.353	ASP89, PRO87, ILE86, GLY85, ARG84, GLY83, ASP81, THR173, ILE175, ILE51, ASN54, SER55, GLU58, LEU103, ILE102, VAL79, GLN91, ARG144
FC-1	-4.218	ASP89, PRO87, ILE86, GLY85, ARG84, ASP81, THR173, ILE175, ILE51, ASN54, SER55, GLU58, LEU103, ILE102, VAL79, GLN91, ARG144
Ofloxacin	-5.107	GLU58, SER55, ASN54, ILE51, PRO87, ILE86, GLY85, ARG84, GLY83, ASP81, THR173, ILE175, VAL131, SER129, SER128, LEU103, ILE102

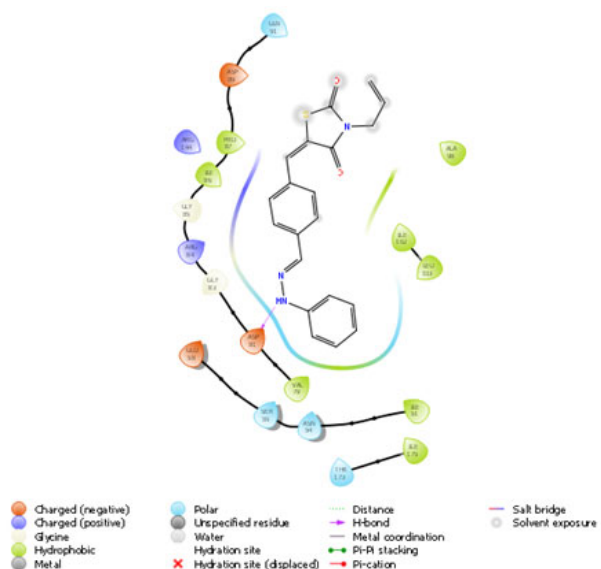
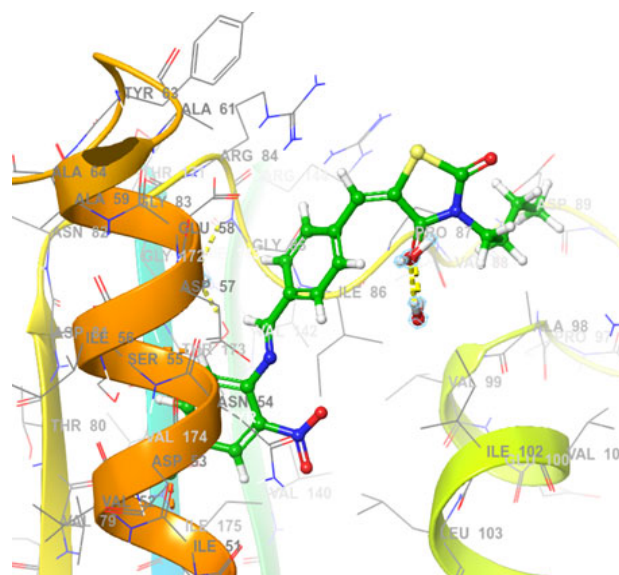




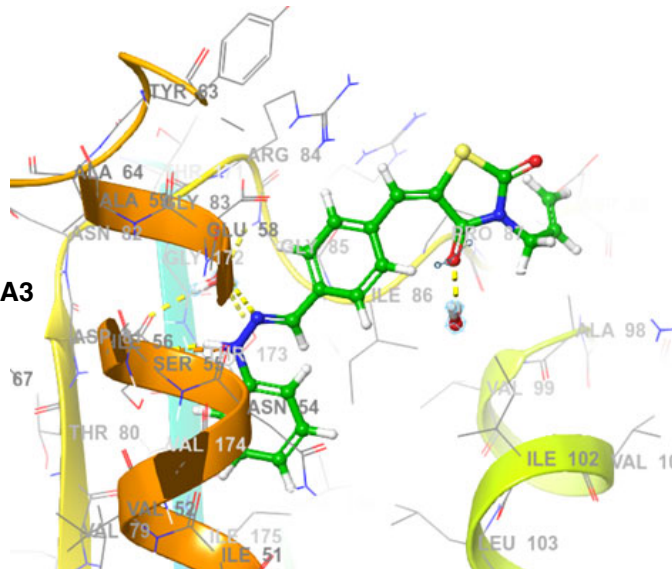
NB20

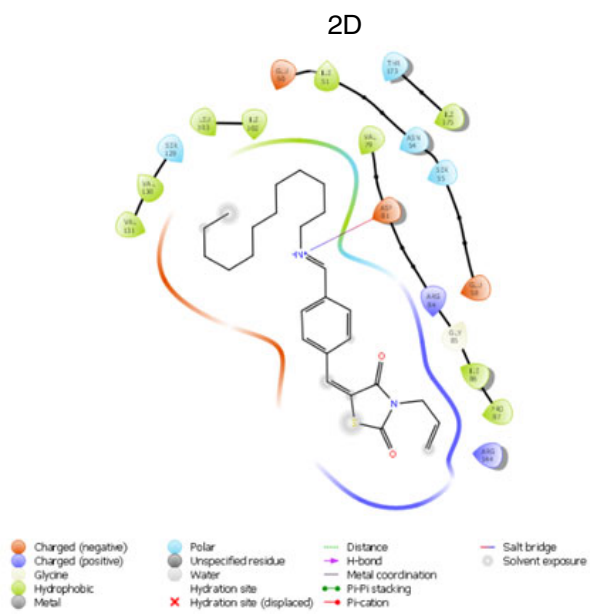


NB14

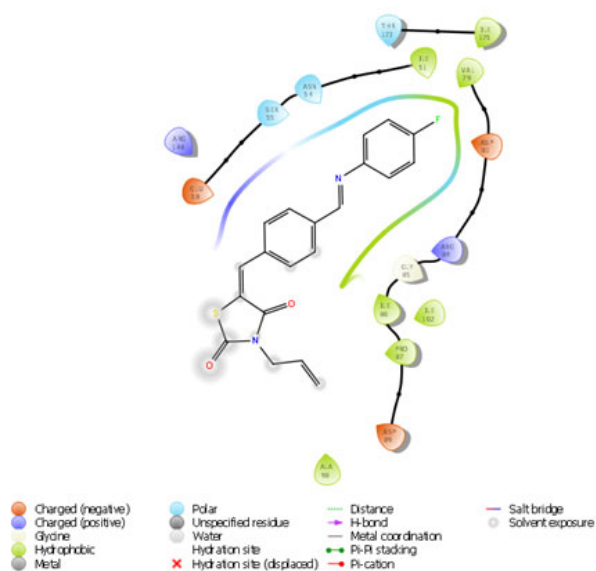
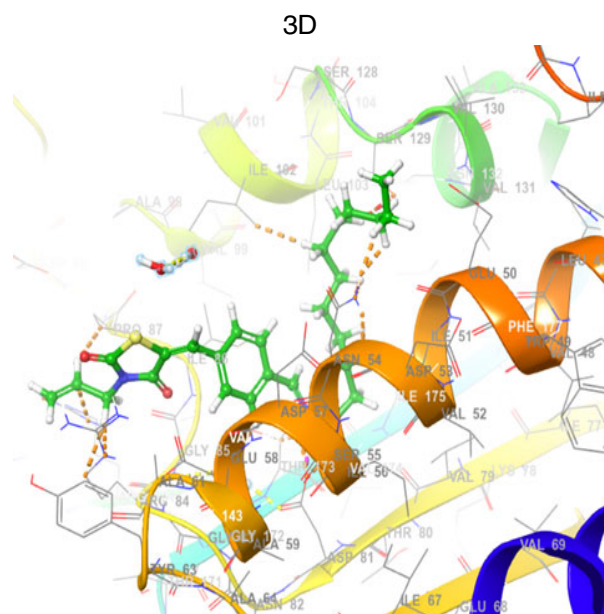


NA3

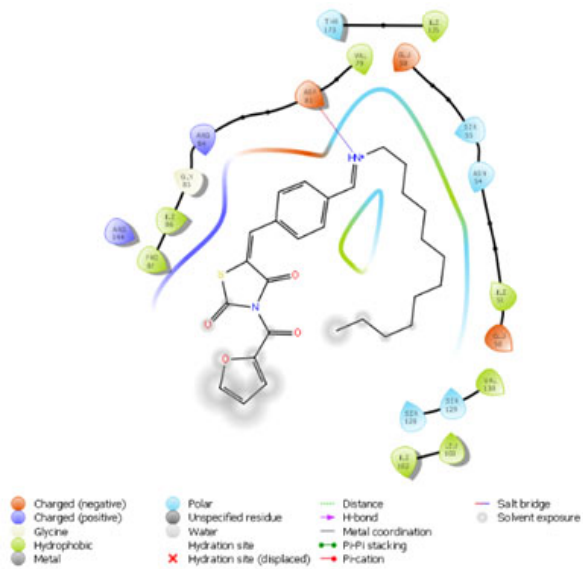
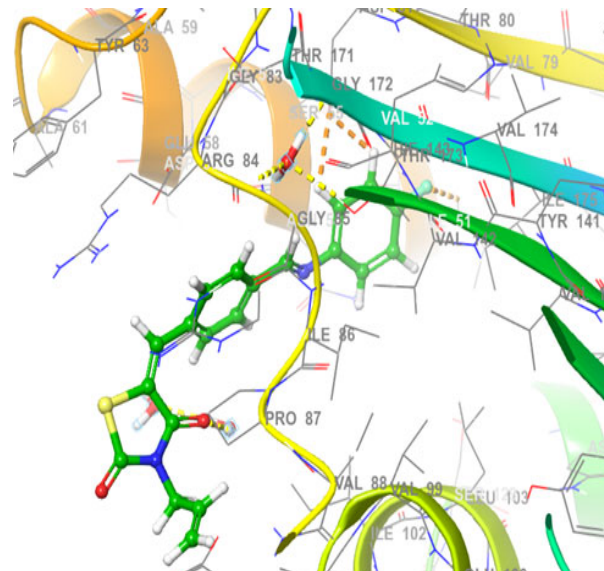




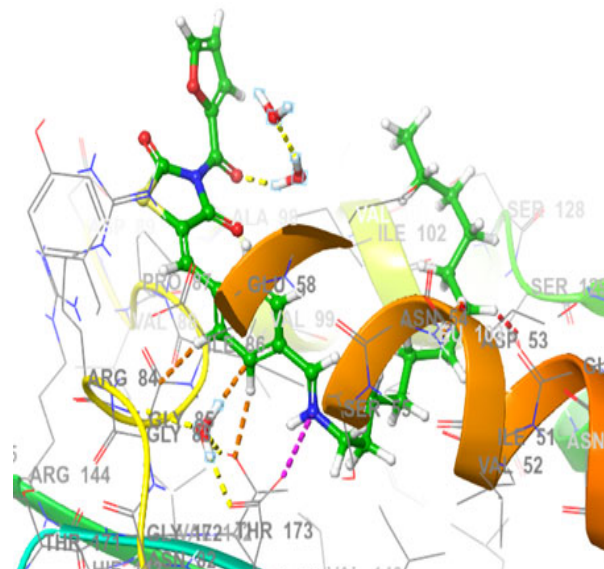
NA20



NA18



FC20



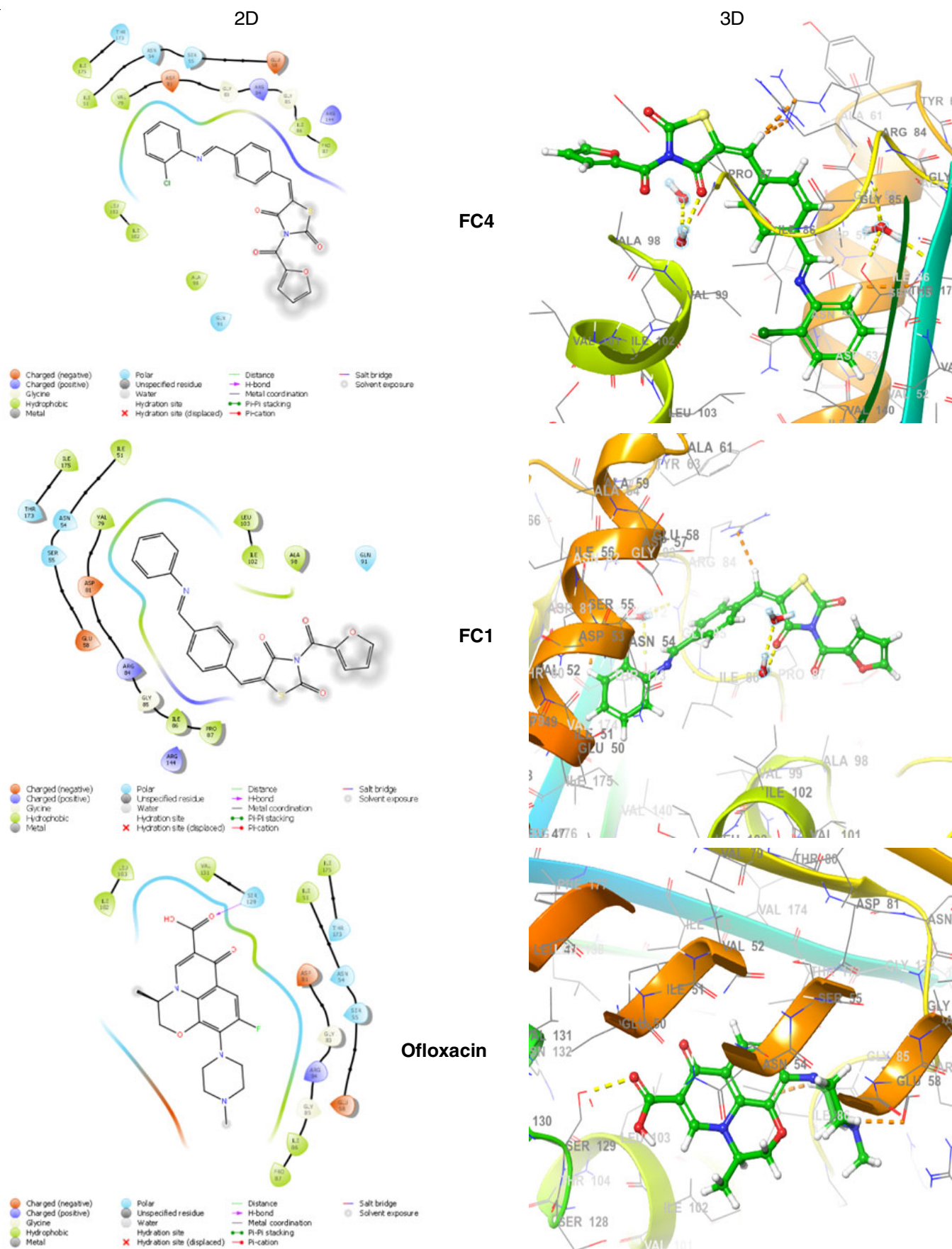
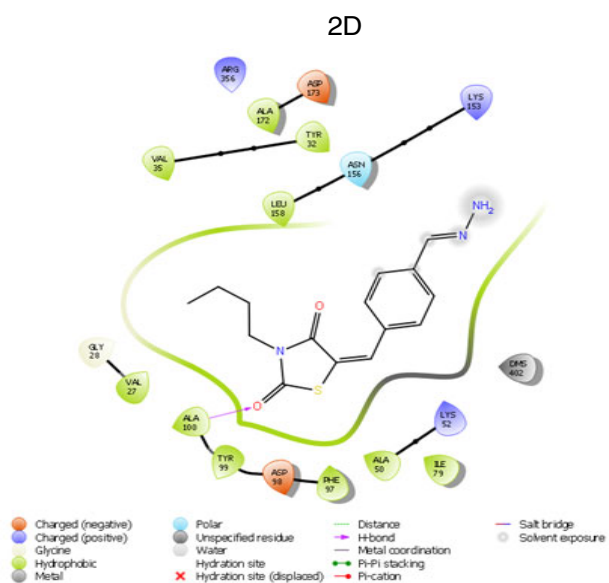


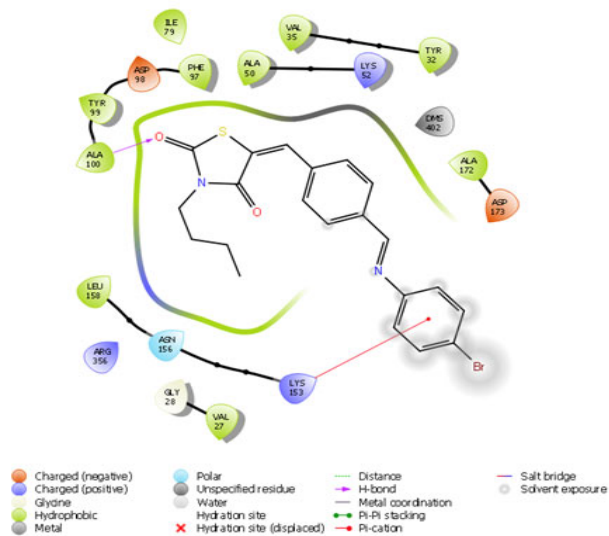
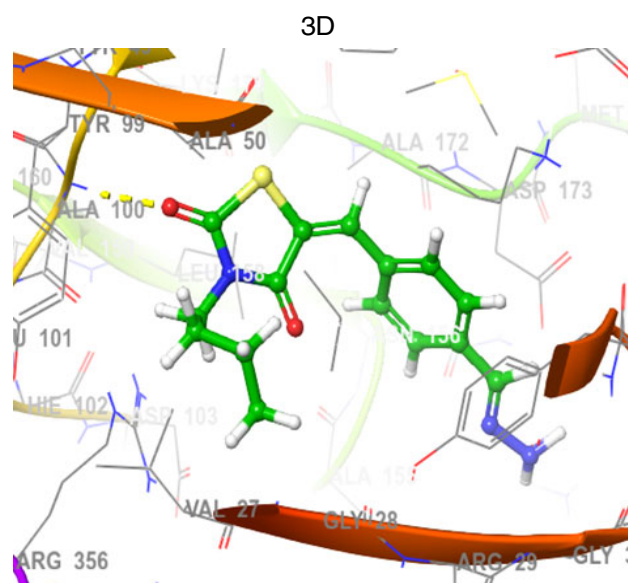
Fig. 1. Interaction of analogue NB3, NB20, NB14, NA3, NA20, NA18, FC20, FC4, FC1 and ofloxacin within the active site of *S. aureus* GyrB ATPase domain protein and interacting amino acid in 2D and 3D view

TABLE-4
DOCKING SCORE AND INTERACTIONS OF MOST ACTIVE COMPOUNDS ALONG WITH
STANDARD DRUG 5-FLUOROURACIL IN THE BINDING POCKET OF 5FGK PROTEIN

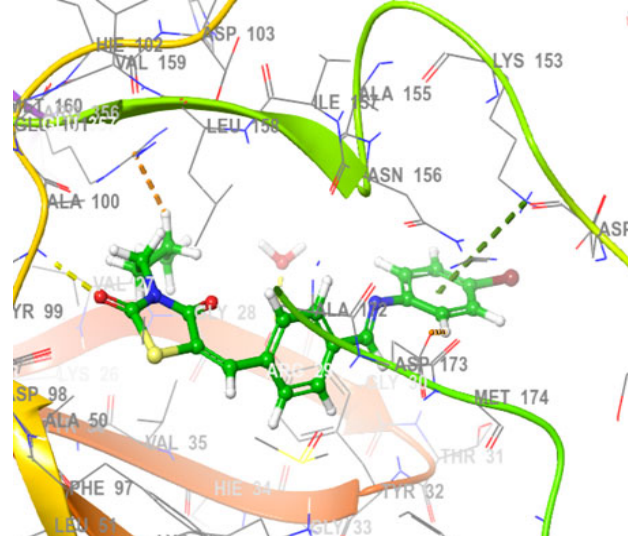
Compound	Docking score	Interacting residues
NA-20	-7.668	VAL27, THR31, TYR32, VAL35, TYR36, ALA50, LYS52, ILE54, GLU55, SER60, SER62, ALA63, GLU66, ILE79, PHE97, ASP98, TYR99, ALA100, LYS153, ASN156, LEU158, ASP173, ALA172, PHE176, ARG356, DMS402, FMT408
NA-2	-7.146	VAL27, GLY28, TYR32, VAL35, ALA50, LYS52, ILE79, PHE97, ASP98, TYR99, ALA100, LEU158, ASP173, ALA172, ARG356, DMS402
NB-2	-6.517	VAL27, GLY28, TYR32, VAL35, ALA50, LYS52, ILE79, PHE97, ASP98, TYR99, ALA100, LYS153, ASN156, LEU158, ASP173, ALA172, ARG356, DMS402
NB-12	-6.502	VAL27, GLY28, TYR32, VAL35, ALA50, LYS52, ILE79, PHE97, ASP98, TYR99, ALA100, LYS153, ASN156, LEU158, ASP173, ALA172, ARG356, DMS402
NB-16	-6.493	VAL27, GLY28, GLY30, TYR32, VAL35, ALA50, LYS52, ILE79, PHE97, ASP98, TYR99, ALA100, ASP151, LYS153, ASN156, LEU158, ASP173, ALA172, ARG356, DMS402
NA-14	-6.141	VAL27, TYR32, VAL35, TYR36, ALA50, LYS52, ILE79, PHE97, ASP98, TYR99, ALA100, LYS153, ASN156, LEU158, ASP173, ALA172, ARG356, DMS402
FC-12	-4.931	VAL27, GLY28, TYR32, VAL35, ALA50, LYS52, ILE79, PHE97, ASP98, TYR99, ALA100, ASP103, ASP151, LYS153, ALA155, ASN156, LEU158, ASP173, ALA172, ARG356, DMS402
FC-11	-4.820	VAL27, GLY28, TYR32, VAL35, ALA50, LYS52, ILE79, PHE97, ASP98, TYR99, ALA100, ASP103, LYS153, ASN156, LEU158, ASP173, ALA172, ARG356, DMS402
FC-9	-4.800	VAL27, GLY28, GLY30, TYR32, VAL35, ALA50, LYS52, ILE79, PHE97, ASP98, TYR99, ALA100, ASP103, ASP151, LYS153, ALA155, ASN156, LEU158, ASP173, ALA172, ARG356, DMS402
5-Fluorouracil	-4.02	VAL27, VAL35, ALA50, ILE79, PHE97, ASP98, TYR99, ALA100, LEU158, ARG356, DMS402

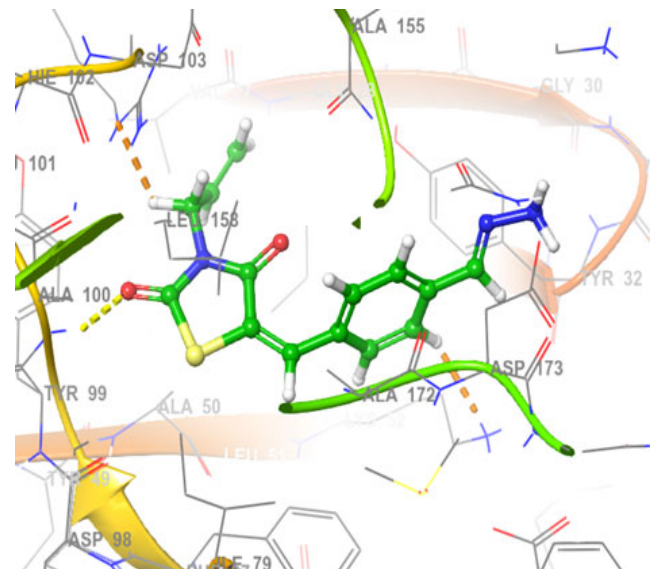
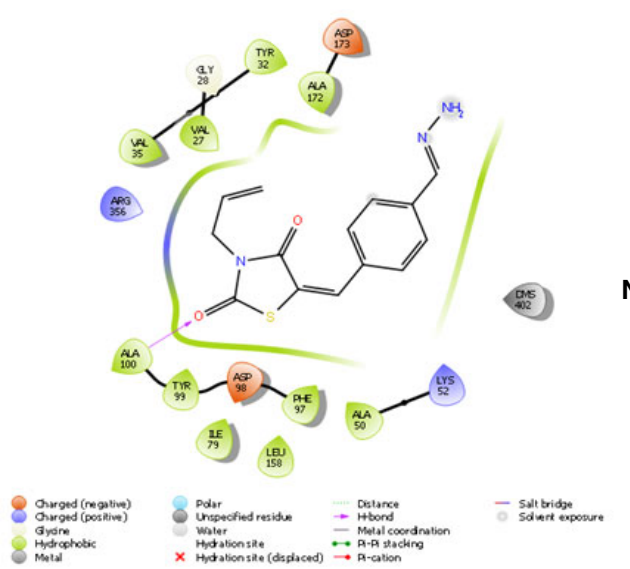
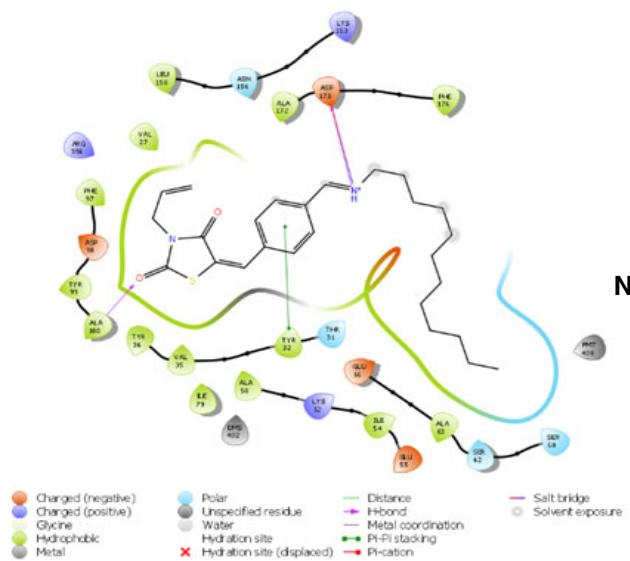
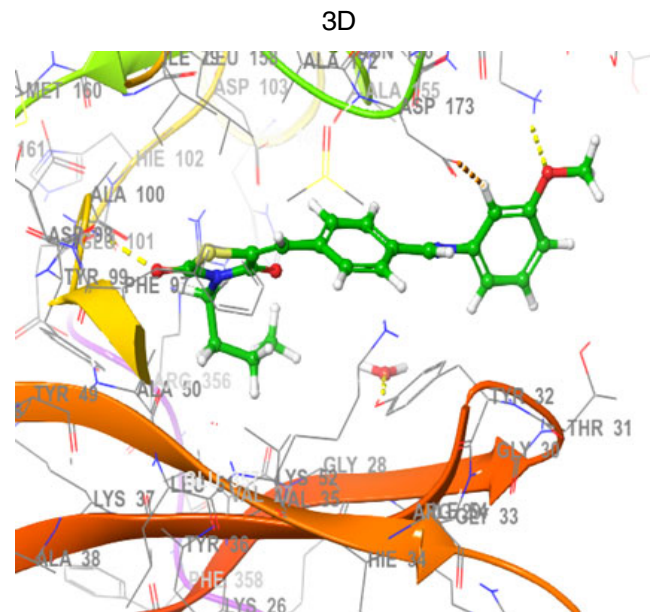
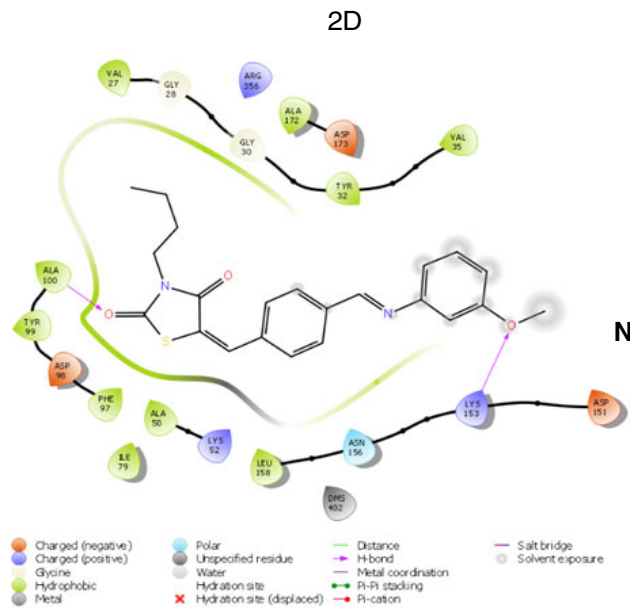


NB2



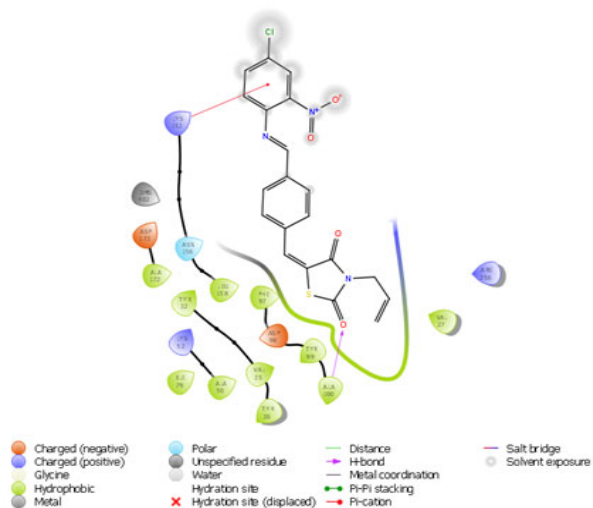
NB12



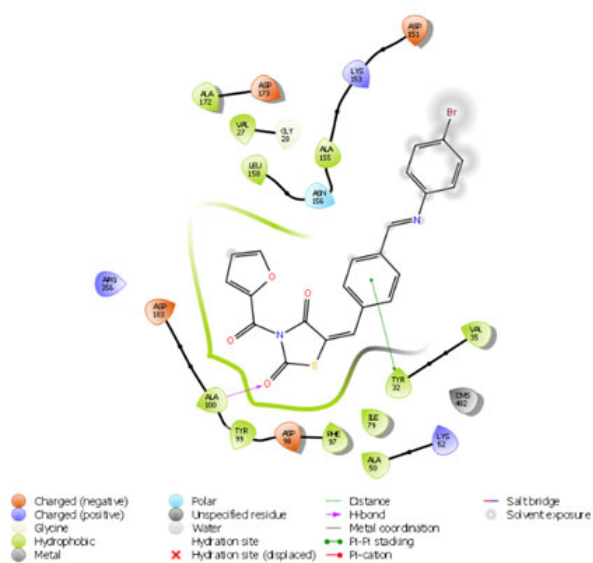
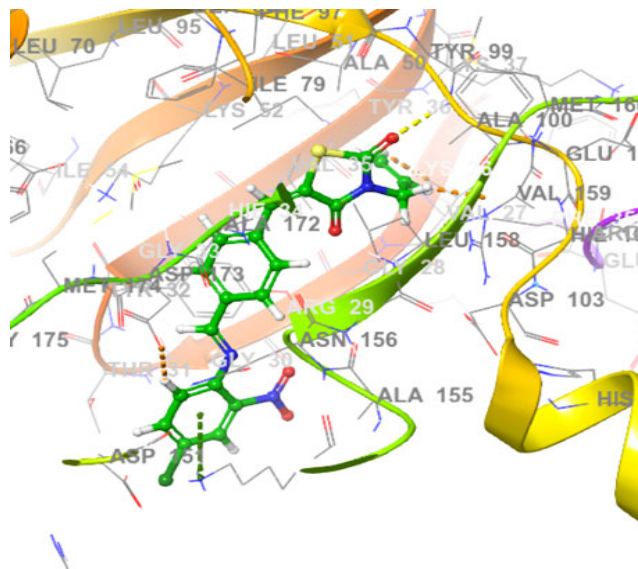


2D

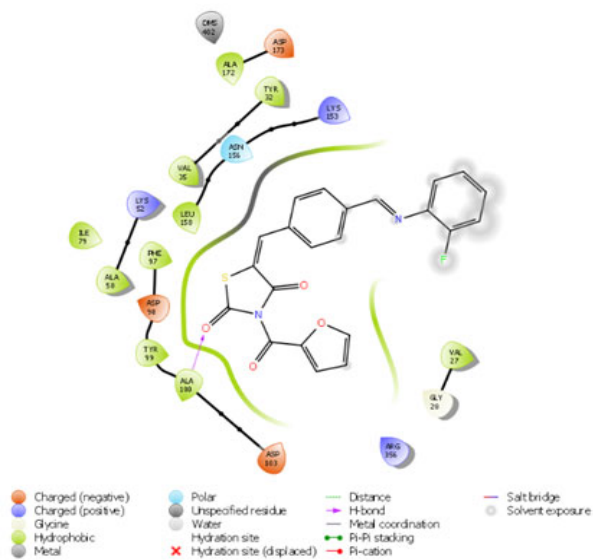
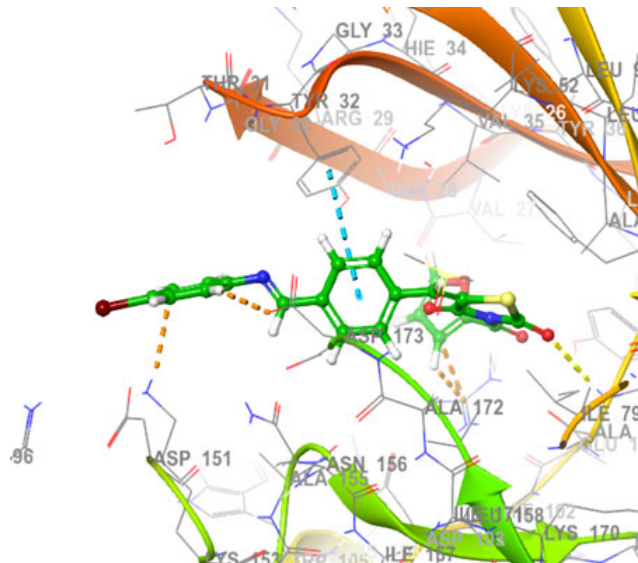
3D



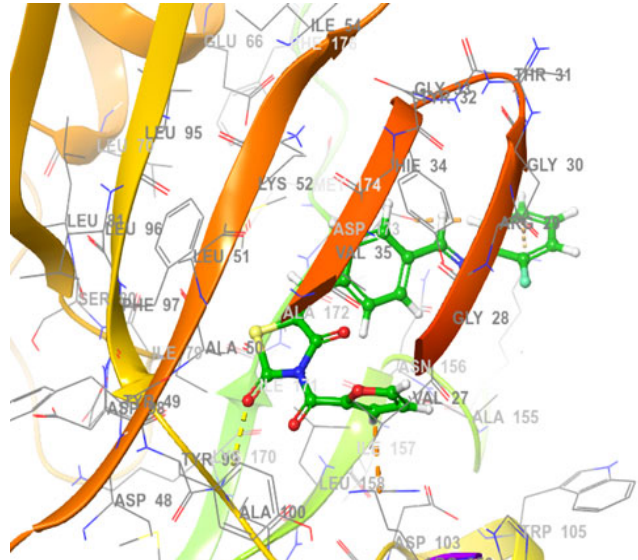
NA14



FC12



FC11



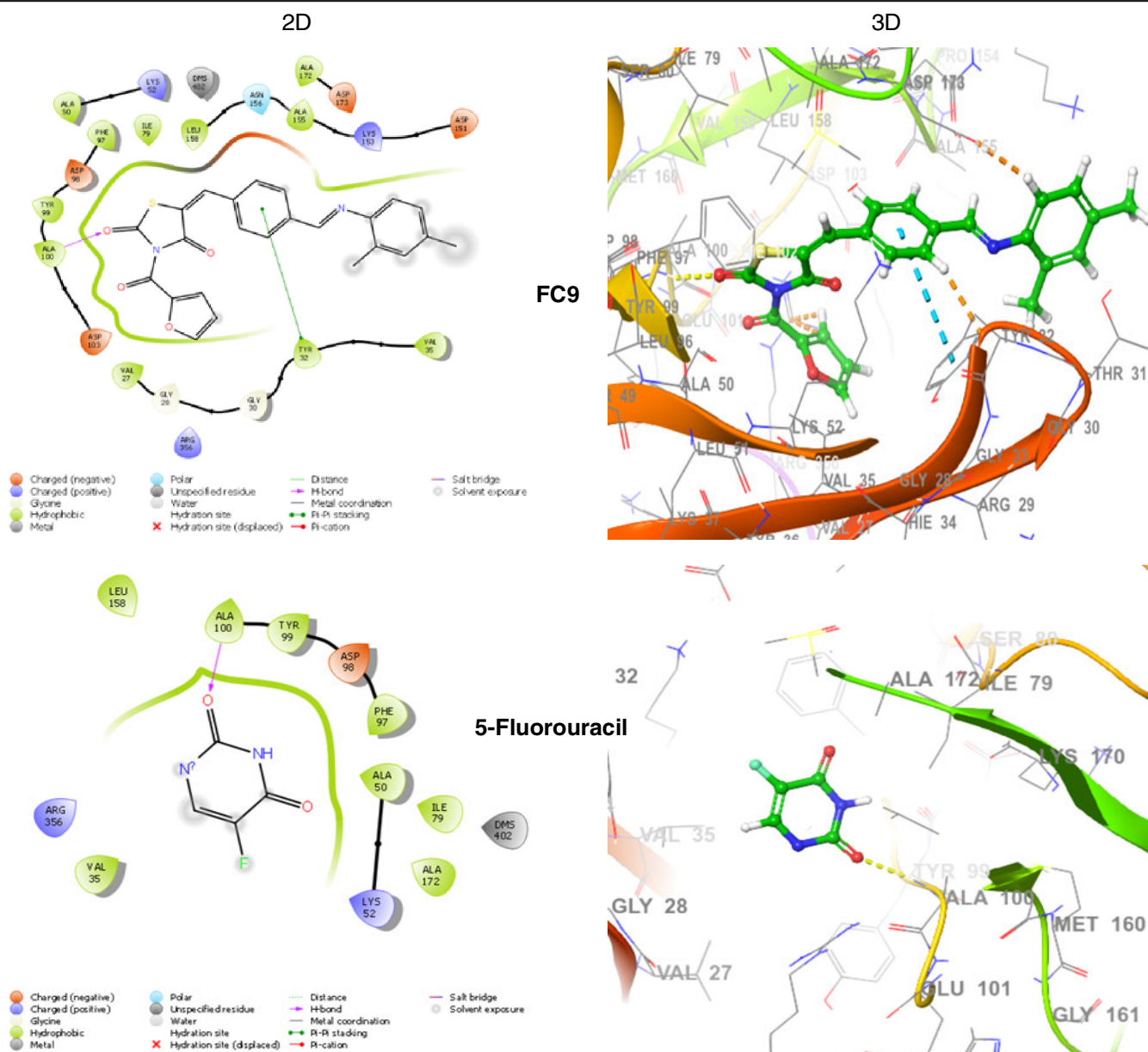


Fig. 2. Interaction of analogue NB2, NB12, NB16, NA20, NA2, NA14, FC12, FC11, FC9 and 5-fluorouracil within the active site of cyclin dependent kinase domain protein and interacting amino acid in 2D and 3D view

and hence these molecules can act as good antimicrobial and antiproliferative molecules. The molecules with furan-2-carbonyl moiety at the 3rd position possessed less docking score in both proteins, which can be due to less interaction of these molecules with crucial amino acids present at the binding site of protein. Further it is revealed from the docking results is that the substitution of dodecyl group or phenyl hydrazine group at 5th position (Schiff base) enhanced the antimicrobial potential. The presence of hydrazine group at 5th position increases the anticancer potential. From the above findings, it is revealed that these molecules can be used as lead for the development of newer antimicrobial/antiproliferative agents with less toxicity.

Conclusion

In present study, data set comprising of 60 compounds was designed and molecular docking analysis was performed

using GLIDE module of Schrödinger software (Maestro version 13.2) to find out the ligand-protein interactions and to find out best stable conformation of each ligand in ligand-protein complex against human cyclin-dependent kinase (5FGK) and *S. aureus* GyrB ATPase (3U2D) proteins. The docking results exhibited that the most molecules possessed better docking score and good interactions towards the binding pocket of protein and are comparable to standard drugs except FC molecules, which possess less interactions hence less docking score. All the molecules exhibited good ADME properties within the range of Qikprop module and also within permissive limits of Lipinski's rule of five and hence make these molecules as suitable drug candidates with better oral bioavailability.

ACKNOWLEDGEMENTS

The authors are thankful to The Head, Department of Pharmaceutical Sciences, Maharshi Dayanand University,

Rohtak, India for providing necessary facilities to carry out this research work.

CONFLICT OF INTEREST

The authors declare that there is no conflict of interests regarding the publication of this article.

REFERENCES

- S.A. Muhammad and N. Fatima, *Pharmacogn. Mag.*, **11**, 123 (2015); <https://doi.org/10.4103/0973-1296.157712>
- L.G. Ferreira, R.N. dos Santos, G. Oliva and A.D. Andricopulo, *Molecules*, **20**, 13384 (2015); <https://doi.org/10.3390/molecules200713384>
- T N Thompson, *Curr. Drug. Metab.*, **1**, 215 (2000); <https://doi.org/10.2174/1389200003339018>
- F. Wu, Y. Zhou, L. Li, X. Shen, G. Chen, X. Wang, X. Liang, M. Tan and Z. Huang, *Front Chem.*, **8**, 726 (2020); <https://doi.org/10.3389/fchem.2020.00726>
- M.A. Salem, A. Ragab, A. El-Khalafawy, A.H. Makhlof, A.A. Askar and Y.A. Ammar, *Bioorg. Chem.*, **96**, 103619 (2020); <https://doi.org/10.1016/j.bioorg.2020.103619>
- M. Durcik, P. Tammela, M. Baranòková, T. Tomašič, J. Ilaš, D. Kikelj and N. Zidar, *ChemMedChem*, **13**, 186 (2018); <https://doi.org/10.1002/cmdc.201700549>
- S.B. Korrapati, P. Yedla, G.G. Pillai, F. Mohammad, P. Bhamidipati, V.R.R. Ch, R. Amanchy, R. Syed and A. Kamal, *Biomed. Pharmacother.*, **134**, 111132 (2021); <https://doi.org/10.1016/j.biopha.2020.111132>
- W. Dan and J. Dai, *Eur. J. Med. Chem.*, **187**, 111980 (2020); <https://doi.org/10.1016/j.ejmech.2019.111980>
- E.A. Fayed, E.S. Nosseir, A. Atef and S.A. El-Kalyoubi, *Mol. Divers.*, **26**, 341 (2022); <https://doi.org/10.1007/s11030-021-10224-4>
- T.S. Ibrahim, A.J. Almalki, A.H. Moustafa, R.M. Allam, G.E.A. Abu-Rahma, H.I. El Subbagh and M.F.A. Mohamed, *Bioorg. Chem.*, **111**, 104885 (2021); <https://doi.org/10.1016/j.bioorg.2021.104885>
- A. Aboelmagd, S.M. El Rayes, M.S. Gomaa, W. Fathalla, I.A.I. Ali, M.S. Nafie, F.H. Pottoo, F.A. Khan and M.M. Ibrahim, *ACS Omega*, **6**, 5244 (2021); <https://doi.org/10.1021/acsomega.0c05263>
- S. Osman, E. Mohammad, M. Lidschreiber, A. Stuetzer, F.L. Bazsó, K.C. Maier, H. Urlaub and P. Cramer, *J. Biol. Chem.*, **296**, 100734 (2021); <https://doi.org/10.1016/j.jbc.2021.100734>
- M. Kumafuji, H. Umemura, T. Furumoto, R. Fukasawa, A. Tanaka and Y. Ohkuma, *Genes Cells*, **19**, 582 (2014); <https://doi.org/10.1111/gtc.12155>
- Y.C. Li, T.C. Chao, H.J. Kim, T. Cholko, S.F. Chen, G. Li, L. Snyder, K. Nakanishi, C.E. Chang, K. Murakami, B.A. Garcia, T.G. Boyer and K.L. Tsai, *Sci. Adv.*, **7**, eabd 4484 (2021); <https://doi.org/10.1126/sciadv.abd4484>
- M.V. Dannappel, D. Sooraj, J.J. Loh and R. Firestein, *Front. Cell Dev. Biol.*, **6**, 171 (2019); <https://doi.org/10.3389/fcell.2018.00171>
- P. Czodrowski, A. Mallinger, D. Wienke, C. Esdar, O. Pöschke, M. Busch, F. Rohdich, S.A. Eccles, M.J. Ortiz-Ruiz, R. Schneider, F.I. Raynaud, P.A. Clarke, D. Musil, D. Schwarz, T. Dale, K. Urbahns, J. Blagg and K. Schiemann, *J. Med. Chem.*, **59**, 9337 (2016); <https://doi.org/10.1021/acs.jmedchem.6b00597>
- H. Kumar, A. Deep and R.K. Marwaha, *BMC Chem.*, **14**, 25 (2020); <https://doi.org/10.1186/s13065-020-00678-2>
- A.P.G. Macabeo, L.A.E. Pilapil, K.Y.M. Garcia, M.T.J. Quimque, C. Phukhamsakda, A.J.C. Cruz, K.D. Hyde and M. Stadler, *Molecules*, **25**, 965 (2020); <https://doi.org/10.3390/molecules25040965>
- S. Tahlan, S. Kumar, K. Ramasamy, S.M. Lim, S.A.A. Shah, V. Mani and B. Narasimhan, *BMC Chem.*, **13**, 90 (2019); <https://doi.org/10.1186/s13065-019-0608-5>
- L. Schrödinger, QikProp, Schrödinger Software Suite, Schrödinger LLC: New York (2022).
- L. Schrödinger, Ligprep, Schrödinger Software Suite, Schrödinger LLC: New York (2022).
- L. Schrödinger, Receptor Grid Generation, GLIDE, Schrödinger Software Suite, Schrödinger LLC: New York (2022).
- L. Schrödinger, Ligand Docking, GLIDE, Schrödinger Software Suite, Schrödinger LLC: New York (2022).
- E.B. Lenselink, J. Louvel, A.F. Forti, J.P.D. van Veldhoven, H. de Vries, T. Mulder-Krieger, F.M. McRobb, A. Negri, J. Goose, R. Abel, H.W.T. van Vlijmen, L. Wang, E. Harder, W. Sherman, A.P. IJzerman and T. Beuming, *ACS Omega*, **1**, 293 (2016); <https://doi.org/10.1021/acsomega.6b00086>
- R.A. Friesner, R.B. Murphy, M.P. Repasky, L.L. Frye, J.R. Greenwood, T.A. Halgren, P.C. Sanschagrin and D.T. Mainz, *J. Med. Chem.*, **49**, 6177 (2006); <https://doi.org/10.1021/jm051256o>
- A. Deep, J. Singh, M. Kumar, R. Mansuri and G.C. Sahoo, *J. Pharm. Bioallied Sci.*, **8**, 188 (2016); <https://doi.org/10.4103/0975-7406.171682>
- F. Bassyouni, M.E. Hefnawi, A.E. Rashed and M. Abdel Rehim, *Drug Des.*, **6**, 1 (2017); <https://doi.org/10.4172/2169-0138.1000148>